
Knowledge Localization: Mission Not Accomplished? Enter Query Localization!

Yuheng Chen^{1,2}, Pengfei Cao^{1,2}, Yubo Chen^{1,2}, Kang Liu^{1,2}, Jun Zhao^{1,2}

¹ The Laboratory of Cognition and Decision Intelligence for Complex Systems,
Institute of Automation, Chinese Academy of Sciences, Beijing, China

² School of Artificial Intelligence, University of Chinese Academy of Sciences, Beijing, China
chenyuheng22@ia.ac.cn, {pengfei.cao, yubo.chen, kliu, jzhao}@nlpr.ia.ac.cn

Abstract

Large language models (LLMs) store extensive factual knowledge, but the mechanisms behind how they store and express this knowledge remain unclear. The Knowledge Neuron (KN) thesis is a prominent theory for explaining these mechanisms. This theory is based on the knowledge localization (KL) assumption, which suggests that a fact can be localized to a few knowledge storage units, namely knowledge neurons. However, this assumption may be overly strong regarding knowledge storage and neglects knowledge expression mechanisms. Thus, we re-examine the KL assumption and confirm the existence of facts that do not adhere to it from both statistical and knowledge modification perspectives. Furthermore, we propose the Query Localization (QL) assumption. (1) Query-KN Mapping: The localization results are associated with the query rather than the fact. (2) Dynamic KN Selection: The attention module contributes to the selection of KNs for answering a query. Based on this, we further propose the Consistency-Aware KN modification method, which improves the performance of knowledge modification. We conduct 39 sets of experiments, along with additional visualization experiments, to rigorously validate our conclusions.

1 Introduction

Large pretrained language models (PLMs) are believed to store extensive factual knowledge [3, 27, 31, 39], however, the mechanisms behind this storage and expression have not been well-explained. The Knowledge Neurons (KN) thesis [4, 5, 7, 10, 22, 23, 26] is a prominent theory aiming to explain these mechanisms. It proposes that PLMs recall facts through their multi-layer perceptron (MLP) weights, referring to the units responsible for storing knowledge as knowledge neurons (KNs). Based on this, KN-inspired model editing methods are proposed [22, 23], which first localize KNs and then modify them to update knowledge, providing further support for the KN thesis.

In fact, the KN thesis is based on the knowledge localization (**KL**) assumption: a piece of factual knowledge can be localized to several KNs. However, this assumption has two issues. (1) In terms of knowledge storage, if we refer to different rephrased queries expressing the same fact as *neighbor queries*, and refer to the corresponding KNs as *neighbor KNs*, then the KL assumption implies that neighbor KNs are consistent. However, as Figure 1 illustrates, while the neighbor KNs of Fact₁ exhibit high consistency, those of Fact₂ show low consistency, indicating the KL assumption does not hold universally. We denote facts that satisfy the KL assumption as **K_I** (e.g., Fact₁), while facts that violate the KL assumption as **K_{II}** (e.g., Fact₂). Previous research and the KL assumption essentially assume that all factual knowledge belongs to K_I. (2) In terms of knowledge expression, the KL assumption only considers how knowledge is stored, without considering how the model selects it to provide answers for queries. Additionally, while components in PLMs are interrelated, the

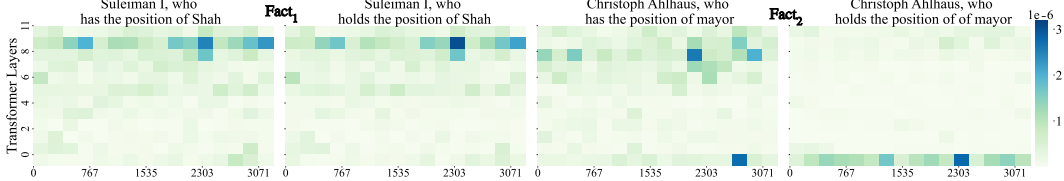


Figure 1: Heatmaps showing the neuron activation values, with darker colors indicating higher activation values. The x -axis and y -axis denote the index and layer of the neurons, respectively. The left two heatmaps show neuron activations for two neighbor queries of $\langle \text{Suleiman I, position, Shah} \rangle$ (Fact₁), while the right two correspond to $\langle \text{Christoph Ahlhaus, position, mayor} \rangle$ (Fact₂). This case employs a representative knowledge localization method [7] in GPT-2.

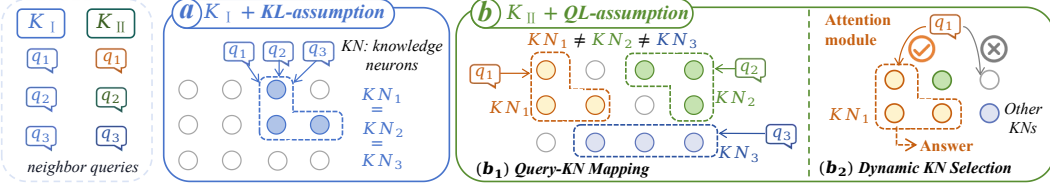


Figure 2: Comparison of the Knowledge Localization (KL) assumption (a) and the Query Localization (QL) assumption (b). Furthermore, the QL assumption is divided into two aspects, as shown in (b₁) and (b₂).

KL assumption focuses on MLP modules while largely ignoring attention modules. Therefore, we re-examine the KL assumption and naturally raise questions Q1 and Q2:

Q1: Does the KL assumption hold for all factual knowledge? If not, is K_{II} widely prevalent? (§2)

A1 We prove the existence of K_{II} that violates the KL assumption from two perspectives. (1) **Statistical Evidence.** As shown in Figures 2(a), if a fact belongs to K_I, its neighbor queries $\{q_1, q_2, q_3\}$ should correspond to the same KNs. Thus, we propose a metric named KN-Consistency Score to evaluate the consistency among neighbor KNs. For a specific fact, a low consistency score indicates that the fact does not belong to K_I. Moreover, to ensure the generalizability of our findings, we employ three advanced knowledge localization methods [4, 7, 10] in three PLMs and conduct significance tests. The results show that for each PLM, a significant proportion of facts consistently belong to K_{II}, regardless of the localization method used. For example, in LLaMA3-8b, this proportion reaches 77%. (2) **Modification-Based Evidence.** We categorize facts into K_I and K_{II} based on their consistency scores to perform knowledge erasure and updates. We find that for facts in K_{II}, editing the KNs corresponding to the query itself does not generalize well to neighbor queries. This indirectly indicates that the neighbor KNs for K_{II} are inconsistent. In summary, the answer to Q1 is: the KL assumption is not always valid and K_{II} is widely prevalent.

Q2: Since the KL assumption has two issues, what is a more realistic assumption? (§3)

A2 To investigate Q2, as shown in Figure 2(b), we introduce the **Query Localization (QL)** assumption, encompassing two aspects. **Query-KN Mapping** (Hypothesis 1): In terms of knowledge storage, for K_{II}, the localization results are associated with the query rather than the fact. For example, in Figure 2(b₁), $\{q_1, q_2, q_3\}$ correspond to three different sets of KNs, i.e., $KN_1 \neq KN_2 \neq KN_3$. **Dynamic KN Selection** (Hypothesis 2). In terms of knowledge expression, the attention module contributes to the selection of KNs for answering a query. As shown in Figure 2(b₂), for K_{II}, facts are distributed and stored across multiple KNs. Since KNs are associated with queries, when confronted with a query q_1 , PLMs leverage the attention module to help select KN_1 to answer q_1 . Notably, the KL assumption is a oversimplification of the QL assumption, where KN_1 to KN_3 happen to overlap.

We validate the QL assumption through three experiments, providing direct and indirect evidence for the two hypotheses. (1) **Query-KN Mapping Demonstration** (direct evidence). For a query, we directly modify the activation values of its corresponding KNs and neighbor KNs. For K_{II}, editing the query's own KNs significantly influences the model's answer to the query, while editing the neighbor KNs has a relatively small impact on the model's answer to the query, which supports

Hypothesis 1. (2) **Dynamic KN Selection Demonstration** (direct evidence). Observing the attention module tends to focus on specific tokens related to the dynamic context of the query, we hypothesize that the attention module contributes to selecting relevant KNs for answering queries in K_{II} . To prove this, we either suppress or enhance attention scores related or unrelated to the query. We find that only query-related attention scores significantly affect KN activation values and the PLMs’ answer probability, which supports Hypothesis 2. (3) **QL-Based Modification** (indirect evidence). Leveraging the QL assumption, we propose the Consistency-Aware KN modification method. Unlike previous methods based directly on localized KNs, we reward high activation values and penalize low consistency KNs to obtain a new set of KNs for editing. The results indicate that the QL assumption can be utilized to improve knowledge modification methods, providing further evidence for its validity. In summary, the answer to Q2 is: A more realistic assumption is the Query Localization assumption.

Our contributions are summarized as follows:

- We conduct the first in-depth exploration of the Knowledge Localization assumption, a foundational assumption of the KN thesis. We show that knowledge not conforming to the KL assumption is prevalent from both statistical and knowledge modification perspectives.
- We propose a more realistic Query Localization assumption, encompassing Query-KN Mapping and Dynamic KN Selection. Based on this assumption, we introduce a Consistency-Aware KN modification method, which outperforms two baselines by an average of 8% and 9% respectively, in the “Erasure” setting on LLaMA3-8b.
- To ensure the rigor of our conclusions, we conduct 39 sets of experiments across 13 experimental settings on 3 PLMs, supplemented by additional visualization experiments.

2 Exploring Knowledge Localization Limitations

This section investigates Q1 and demonstrates the existence of K_{II} , a term referring to knowledge that does not satisfy the knowledge localization assumption. Our experiments adopt GPT-2 [31], LLaMA2-7b [39], and LLaMA3-8b [3], representing a range of sizes of popular auto-regressive models. This allows us to assess the scalability of our methods and conclusions. Consistent with other knowledge localization methods [4, 7, 10], we utilize the fill-in-the-blank cloze task [27] and the ParaRel dataset [9]. For details to the datasets, see Table 5 in A.2.

2.1 Statistical Evidence for the Existence of K_{II}

In this subsection, we prove that the consistency of KNs of some facts is very low, which shows that these facts do not meet the KL assumption.

Consistency Analysis According to the KL assumption, neighbor queries should be localized to the same KNs, with any deviations primarily attributable to the localization method itself. To assess this, we calculate the corresponding KNs for each query and introduce the KN-Consistency Score (CS) metric. Given a fact with k neighbor queries $\{q_1, \dots, q_k\}$, we calculate its CS as follows:

$$CS_1 = \frac{|\bigcap_{i=1}^k \mathcal{N}_i|}{|\bigcup_{i=1}^k \mathcal{N}_i|} \quad \xrightarrow{\text{relaxation}} \quad CS_2 = \frac{|\{n \mid n \in \bigcup_{i=1}^k \mathcal{N}_i \text{ and } \sum_{i=1}^k \mathbb{1}_{n \in \mathcal{N}_i} > 1\}|}{|\bigcup_{i=1}^k \mathcal{N}_i|} \quad (1)$$

where \mathcal{N}_i are the KNs corresponding to query q_i , n is a KN. CS_1 requires n to appear in all \mathcal{N}_i , while its relaxed version, CS_2 , only requires n to appear in more than one \mathcal{N}_i . Therefore, CS_2 effectively reduces the impact of errors in the localization method, providing stronger evidence for the existence of K_{II} . Then, we use a thresholding technique based on CS_2 , classifying facts above a certain threshold as K_I and those below it as K_{II} . We consider two types of thresholds: a static threshold and Otsu’s threshold [1]. While Otsu’s threshold aims to maximize the between-class variance and effectively separate two classes of data, the static threshold reflects the inherent nature of a fact’s adherence (or non-adherence) to the KL assumption. See Table 4 in A.1 for specific thresholds. Furthermore, to ensure our findings are not method-specific, we employ three advanced knowledge localization methods for comparison [4, 7, 10] (detailed in A.4). Finally, we apply Welch’s t-test [2] to confirm the statistical significance of the difference between K_I and K_{II} .

Table 1: Overall results of Consistency Analysis. We consider three PLMs along with three different knowledge localization methods. The symbol T represents the static threshold (St) and Otsu threshold (Ot). The terms “R: I”, “S: I”, “R: II”, and “S: II” represent the ratios and KN-consistency scores for K_I and K_{II} , respectively. The t -statistics and p -value for the T-test conducted on K_I and K_{II} are denoted as t and p . In all cases, $p < 1e - 6$. “ \cap : II” represents the proportion of facts classified as K_{II} by all three knowledge localization methods.

| GPT-2 | | | | | | | | | | | | | | | | |
|-----------|----------------|------|-------------|-------|-----|----------------|------|-------------|-------|-----|-----------------|------|-------------|-------|-----|-------------|
| T | Dai et al. [7] | | | | | Enguehard [10] | | | | | Chen et al. [4] | | | | | |
| | R: I | S: I | R: II | S: II | t | R: I | S: I | R: II | S: II | t | R: I | S: I | R: II | S: II | t | \cap : II |
| St | 0.56 | 0.21 | 0.44 | 0.03 | 236 | 0.54 | 0.23 | 0.46 | 0.03 | 235 | 0.53 | 0.25 | 0.47 | 0.03 | 230 | 0.42 |
| Ot | 0.41 | 0.24 | 0.59 | 0.06 | 223 | 0.44 | 0.29 | 0.55 | 0.05 | 219 | 0.40 | 0.29 | 0.60 | 0.06 | 221 | 0.53 |
| LLaMA2-7b | | | | | | | | | | | | | | | | |
| T | Dai et al. [7] | | | | | Enguehard [10] | | | | | Chen et al. [4] | | | | | |
| | R: I | S: I | R: II | S: II | t | R: I | S: I | R: II | S: II | t | R: I | S: I | R: II | S: II | t | \cap : II |
| St | 0.40 | 0.21 | 0.60 | 0.04 | 158 | 0.39 | 0.20 | 0.61 | 0.04 | 150 | 0.40 | 0.20 | 0.60 | 0.04 | 160 | 0.55 |
| Ot | 0.21 | 0.28 | 0.79 | 0.062 | 152 | 0.20 | 0.25 | 0.80 | 0.07 | 158 | 0.24 | 0.30 | 0.76 | 0.06 | 132 | 0.70 |
| LLaMA3-8b | | | | | | | | | | | | | | | | |
| T | Dai et al. [7] | | | | | Enguehard [10] | | | | | Chen et al. [4] | | | | | |
| | R: I | S: I | R: II | S: II | t | R: I | S: I | R: II | S: II | t | R: I | S: I | R: II | S: II | t | \cap : II |
| St | 0.16 | 0.16 | 0.84 | 0.03 | 114 | 0.15 | 0.18 | 0.85 | 0.03 | 105 | 0.18 | 0.19 | 0.82 | 0.03 | 123 | 0.77 |
| Ot | 0.23 | 0.14 | 0.77 | 0.03 | 128 | 0.21 | 0.15 | 0.79 | 0.03 | 107 | 0.24 | 0.16 | 0.76 | 0.03 | 130 | 0.70 |

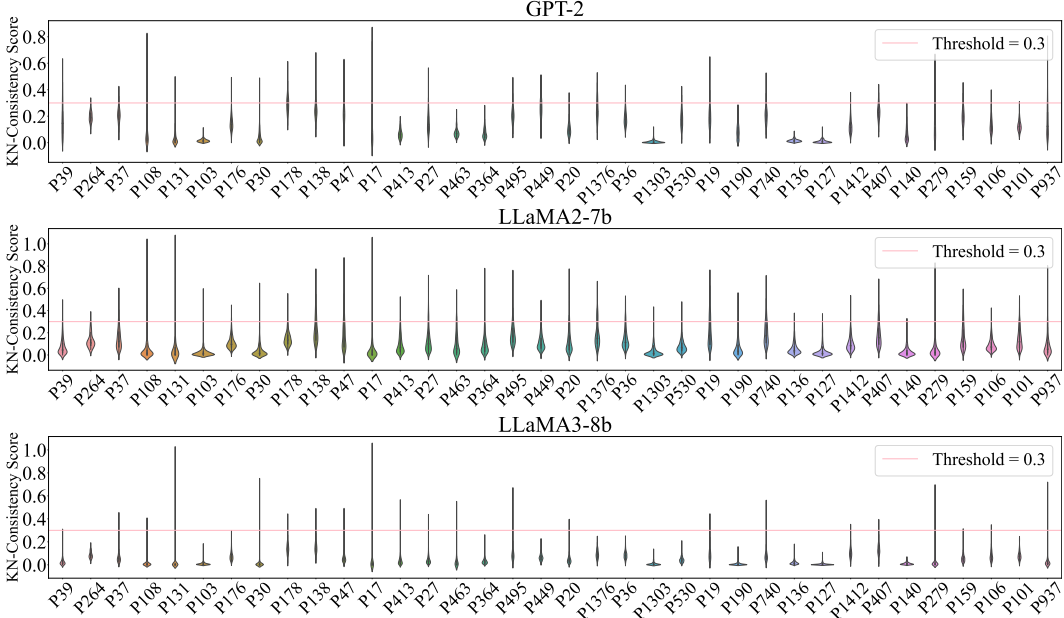


Figure 3: Violin plot for Consistency Analysis. The x -axis represents the fact relations, and the y -axis denotes the CS_2 values. The width of each violin plot indicates the density of data at different CS_2 values. We select a threshold of 0.3 as an example, and facts below this threshold are classified as K_{II} .

Findings Figure 3 classifies facts by their respective relations and displays the distribution of CS_2 when utilizing the knowledge localization method of Dai et al. [7]. The violin plots for two other methods are presented in Figures 8 and 9 in A.3. Additionally, Table 1 summarizes the overall results. These results lead to the following conclusions: (1) K_{II} exists extensively. Table 1 shows a consistently high ratio of K_{II} (R: II) and low CS values (S: II), regardless of the knowledge localization method or threshold used. The proportion of facts consistently categorized as K_{II} across different methods is also high (\cap : II). Figure 3, using an example threshold of 0.3, reveals that the majority of facts across various relations fall below this threshold, thus belonging to K_{II} . (2) The difference between

K_I and K_{II} is significant. Significance test results consistently show high t -statistics and low p -values, confirming a highly significant difference in all cases. (3) The larger the PLMs, the more extensively K_{II} exists. As shown in Table 1, in larger PLMs, the proportion of K_{II} is higher and the CS values are lower. This phenomenon is also observed for most relations in Figure 3. This is understandable as larger models, with more parameters, are more likely to store a single fact across multiple neurons.

2.2 Modification-Based Evidence for the Existence of K_{II}

In this subsection, we conduct knowledge modification experiments to demonstrate the existence of K_{II} . We use a static threshold to classify facts into K_I and K_{II} .

Experimental setups Let $\langle s, r, o \rangle$ denote a fact consisting of a subject (s), relation (r), and object (o). We perform two types of knowledge modification: Erasure and Update. Given a fact with k queries, and for a query q_i , modify the MLP weights of the PLMs as follows.

$$\text{For } \forall [l, p] \in \begin{cases} \mathcal{N}_i, & \text{if Local set} \\ \mathcal{N}_g = \bigcup_{j=1}^k \mathcal{N}_j, & \text{if Global set} \end{cases}, \quad W_{l,p} = \begin{cases} 0, & \text{if Erasure} \\ W_{l,p} - \lambda_1 E(o) + \lambda_2 E(o'), & \text{if Update} \end{cases} \quad (2)$$

where l and p represent the layer and position of the KN, $W_{l,p}$ is the MLP weight at $[l, p]$. \mathcal{N}_i is the set of KNs corresponding to q_i (Local set), while \mathcal{N}_g is the union of KNs across all queries (Global set). $E(o)$ and $E(o')$ are the word embeddings of the original object o and the updated object o' , respectively. λ_1 and λ_2 are hyperparameters.

Evaluation Metrics We used two types of evaluation perspectives. (1) *Knowledge Modification Metrics*: We adopt three metrics: Reliability, Generalization, and Locality [43] (detailed in A.5), but with some modifications. After erasing a fact (Erasure), we assess the model’s ability to answer the query q_i and neighbor queries $q_N = \{q_j \mid j \neq i\}$. Low reliability and generalization indicate successful erasure, while high locality indicates other facts remain unaffected. For the former two metrics, we invert their values (i.e., 1 - value) to align with the positive direction of improvement. After updating a fact (Update), we assess the model’s ability to answer the new query belonging to $\langle s', r, o' \rangle$, all three metrics are better when higher. (2) *General Capability Metrics*: Editing neurons may disrupt the model’s performance in generating text [44, 45]. Similar to other model editing methods [41], we employ the perplexity (PPL) metric to evaluate the model’s general capability after modification. Specifically, we randomly select five entries from WikiText2 [24] each time and calculate the relative increase in PPL before (b) and after (a) editing the model: $\Delta\text{PPL} = \frac{\text{PPL}_a - \text{PPL}_b}{\text{PPL}_b}$.

Findings Table 2 presents the results of this experiment, leading us to the following conclusions: (1) For K_{II} , modifying \mathcal{N}_i (Local set) results in a low generalization, indicating unsuccessful modification of neighbor queries. In contrast, for K_I , both “Avg” and “Gen” metrics are higher than those of K_{II} . This suggests higher consistency among neighbor KNs for K_I , while neighbor KNs for K_{II} are highly inconsistent. (2) For K_{II} , we must modify \mathcal{N}_g (Global set) to ensure high generalization, meaning we must modify numerous KNs to erase or update a single fact. However, this also leads to a high ΔPPL , indicating excessive alteration of model parameters. This suggests that the fact cannot be localized to a few KNs. Taken together, (1) and (2) confirm that K_{II} does not adhere to the KL assumption.

3 Query Localization Assumption

Motivation Since K_{II} does not satisfy the KL assumption, we naturally raise question Q2: What is a more realistic assumption? Tables 1 and 2 suggest that for K_{II} , KNs might relate to queries rather than facts. Then, we further consider: if a fact is stored across many KNs, how does the model select the appropriate set of KNs to answer queries correctly? The KL assumption only considers how MLP stores knowledge, without considering how the model selects KNs for answering. In light of research on the attention module [12, 22, 32], we argue that it should be considered and hypothesize that it plays a role in selecting KNs. In summary, we propose the Query Localization (QL) assumption, which includes two aspects. Query-KN Mapping (Hypothesis 1): For K_{II} , the localization results are associated with the query rather than the fact. Dynamic KN Selection (Hypothesis 2): For a specific query, the attention module contributes to the selection of KNs for answering a query. In fact, the KL assumption can be considered as a simplification of the QL assumption when KNs happen to

Table 2: Results of Knowledge Modification. We consider three PLMs and two types of knowledge. “Erasure” and “Update” represent our two operations performed. \mathcal{N}_i and \mathcal{N}_g are the two sets of KNs. “Rel”, “Gen”, and “Loc” stand for reliability, generalization, and locality metrics, respectively; “Avg” represents the average value, each of which are better when higher. “ ΔPPL ” denotes the change of perplexity, which is better when lower.

| <i>Erasure</i> | | | | | | | | | | | | | | | |
|-----------------|--------------|------|------|------|--------------|------------------|------|------|------|--------------|------------------|------|------|------|--------------|
| \mathcal{N}_i | GPT-2 | | | | | LLaMA2-7b | | | | | LLaMA3-8b | | | | |
| | Rel | Gen | Loc | Avg | ΔPPL | Rel | Gen | Loc | Avg | ΔPPL | Rel | Gen | Loc | Avg | ΔPPL |
| K_I | 0.55 | 0.47 | 0.93 | 0.65 | 0.02 | 0.33 | 0.34 | 0.79 | 0.49 | 0.01 | 0.28 | 0.30 | 0.83 | 0.47 | 0.04 |
| K_{II} | 0.50 | 0.09 | 0.97 | 0.52 | 0.06 | 0.36 | 0.11 | 0.80 | 0.42 | 0.03 | 0.34 | 0.04 | 0.90 | 0.43 | 0.05 |
| <i>Update</i> | | | | | | | | | | | | | | | |
| \mathcal{N}_i | GPT-2 | | | | | LLaMA2-7b | | | | | LLaMA3-8b | | | | |
| | Rel | Gen | Loc | Avg | ΔPPL | Rel | Gen | Loc | Avg | ΔPPL | Rel | Gen | Loc | Avg | ΔPPL |
| K_I | 0.53 | 0.40 | 0.99 | 0.64 | 0.04 | 0.30 | 0.39 | 0.89 | 0.53 | 0.03 | 0.30 | 0.29 | 0.79 | 0.46 | 0.07 |
| K_{II} | 0.44 | 0.11 | 0.96 | 0.50 | 0.09 | 0.39 | 0.07 | 0.80 | 0.42 | 0.08 | 0.29 | 0.08 | 0.86 | 0.41 | 0.08 |
| <i>Erasure</i> | | | | | | | | | | | | | | | |
| \mathcal{N}_g | GPT-2 | | | | | LLaMA2-7b | | | | | LLaMA3-8b | | | | |
| | Rel | Gen | Loc | Avg | ΔPPL | Rel | Gen | Loc | Avg | ΔPPL | Rel | Gen | Loc | Avg | ΔPPL |
| K_I | 0.58 | 0.55 | 0.90 | 0.68 | 0.12 | 0.30 | 0.55 | 0.70 | 0.52 | 0.08 | 0.30 | 0.35 | 0.80 | 0.48 | 0.18 |
| K_{II} | 0.65 | 0.60 | 0.70 | 0.65 | 2.02 | 0.44 | 0.45 | 0.52 | 0.42 | 1.50 | 0.36 | 0.40 | 0.50 | 0.49 | 1.05 |
| <i>Update</i> | | | | | | | | | | | | | | | |
| \mathcal{N}_g | GPT-2 | | | | | LLaMA2-7b | | | | | LLaMA3-8b | | | | |
| | Rel | Gen | Loc | Avg | ΔPPL | Rel | Gen | Loc | Avg | ΔPPL | Rel | Gen | Loc | Avg | ΔPPL |
| K_I | 0.56 | 0.48 | 0.88 | 0.64 | 0.13 | 0.32 | 0.59 | 0.82 | 0.68 | 0.10 | 0.44 | 0.41 | 0.74 | 0.53 | 0.22 |
| K_{II} | 0.54 | 0.55 | 0.74 | 0.61 | 1.88 | 0.40 | 0.43 | 0.62 | 0.48 | 1.16 | 0.29 | 0.33 | 0.66 | 0.43 | 0.93 |

overlap, and it is entirely feasible to analyze K_I using the QL assumption. Moreover, the proof of the QL assumption can further illustrate the issues of the KL assumption. Below, we divide the facts into K_I and K_{II} to conduct experiments and prove the QL assumption.

3.1 Demonstration of the Query Localization Assumption: Query-KN Mapping

Experimental Settings We first prove the Query-KN Mapping hypothesis. Tables 1 and 2 offer preliminary evidence, and now we directly manipulate KN activation values to reinforce this point. Unlike modifying model parameters, modifying KN activation values directly reflect the impact of KNs on the answer [4, 7]. For a given query q_i , we either suppress or enhance its corresponding KNs \mathcal{N}_i . In contrast, we suppress or enhance the set of its neighbor KNs \mathcal{N}_i^N . Here, we adopt three methods for obtaining \mathcal{N}_i^N .

$$\mathcal{N}_i^N = \begin{cases} \bigcup_{j=1}^k \mathcal{N}_j (j \neq i), & \text{for Union} \\ \bigcap_{j=1}^k \mathcal{N}_j (j \neq i), & \text{for Intersection} \\ \{n \mid n \in \bigcup_{j=1}^k \mathcal{N}_j \text{ and } \sum_{j=1}^k \mathbb{1}(n \in \mathcal{N}_j) > 1\} \quad (j \neq i), & \text{for Refine} \end{cases} \quad (3)$$

where n is a KN, $\sum_{j=1}^k \mathbb{1}(n \in \mathcal{N}_j)$ counts the occurrences of n . Regarding evaluation metrics, we follow the established practice in knowledge localization methods [4, 5, 7, 10], and calculate the rates of increase and decrease in the PLMs’ answer probabilities before (b) and after (a) suppression and enhancement: $\Delta \text{Prob} = \pm \frac{\text{Prob}_a - \text{Prob}_b}{\text{Prob}_b}$, where “+” indicates an increase and “-” a decrease.

Findings Figure 4 demonstrates that the Query-KN Mapping of the QL assumption is established. (1) Regardless of whether it is K_I or K_{II} , the results from the “Self (\mathcal{N}_i)” suggest that the influence of suppressing or enhancing the query’s own KNs is significant. This indicates that the KNs are associated with the query. (2) For K_{II} , the average values (“Avg”) of \mathcal{N}_i^N are much lower than that of \mathcal{N}_i , especially in the strictest “Intersection” case. However, for K_I , the average values decrease less. This indicates that the neighbor KNs for K_I are more consistent, while the neighbor KNs for K_{II} are much less consistent. This shows that for K_{II} , KNs do not correspond to the fact itself. Combining

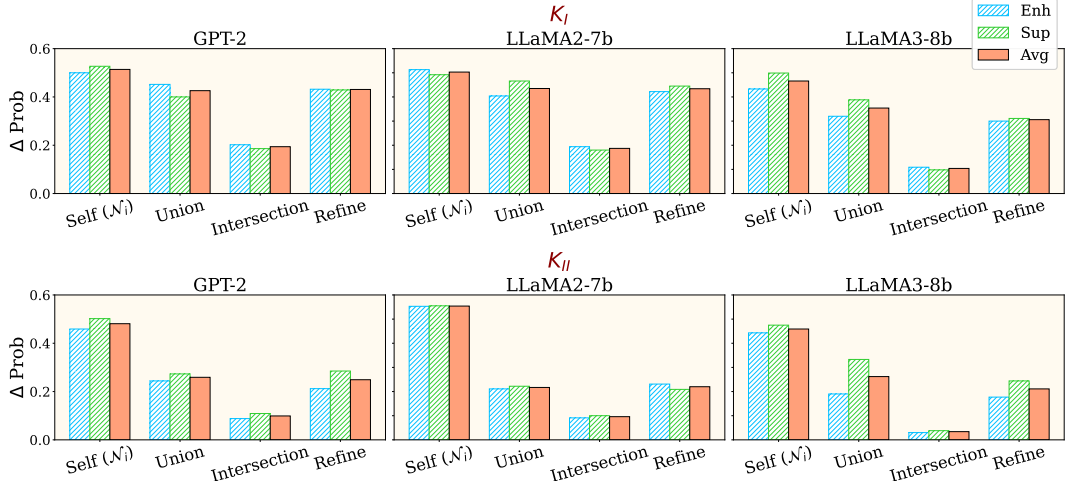


Figure 4: Results of the Query-KN Mapping demonstration experiment. “Self (\mathcal{N}_i)” refers to the KNs associated with a specific query, while the other three scenarios pertain to the neighbor KNs. We adopt three sets for \mathcal{N}_i^N : Union, Intersection, and Refine, which respectively unionize, intersect, and refine the KNs to select those that appear more than once. “Enh” and “Sup” refer to enhancement and suppression of KN activation values, respectively, with “Avg” representing their average. The values in the figure represent ΔProb , the change rate in the model’s answer probabilities before and after modifying KN activation values.

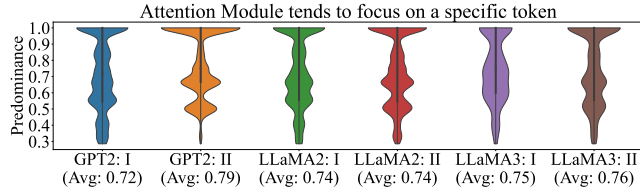


Figure 5: Experimental results of the distribution of the \mathcal{P} values. “I” and “II” represent K_I and K_{II} respectively. For example, “GPT2:I” represents the \mathcal{P} values of facts belonging to K_I under the GPT-2.

(1) and (2), we conclude that KNs are associated with the query rather than the fact, i.e., Query-KN Mapping is established. (3) Furthermore, for K_I , the average values also decrease, indicating that its neighbor KNs are not entirely consistent. Thus, K_I can be considered a special case of K_{II} .

3.2 Demonstration of the Query Localization Assumption: Dynamic KN Selection

In this subsection, we first explain why we propose the Dynamic KN Selection hypothesis, then, we present experimental evidence to support this hypothesis.

3.2.1 Preliminary Analysis of Attention Module

To examine the role of the attention module, we conduct a preliminary experiment. Specifically, we identify the token with the highest attention score and define the predominance score \mathcal{P} . For a fact with k queries $\{q_1, q_2, \dots, q_k\}$, its \mathcal{P} is calculated as follows:

$$A_i^{(r,c)} = \frac{1}{LH} \sum_{l=1}^L \sum_{h=1}^H A_{(l,h)}^{(r,c)} \Rightarrow t_i = q_i[\arg \max_r \sum_c A_i^{(r,c)}] \Rightarrow \mathcal{P} = \max_t \frac{\sum_{i=1}^k \mathbb{1}(t = t_i)}{k} \quad (4)$$

where $A_i^{(r,c)}$ represents the attention score matrix for query q_i , with r and c denoting rows and columns. L and H represent the number of layers and heads of the attention module, t_i is the most attended token for q_i , and $\sum_{i=1}^k \mathbb{1}(t = t_i)$ counts the occurrences of each token. The violin plot in

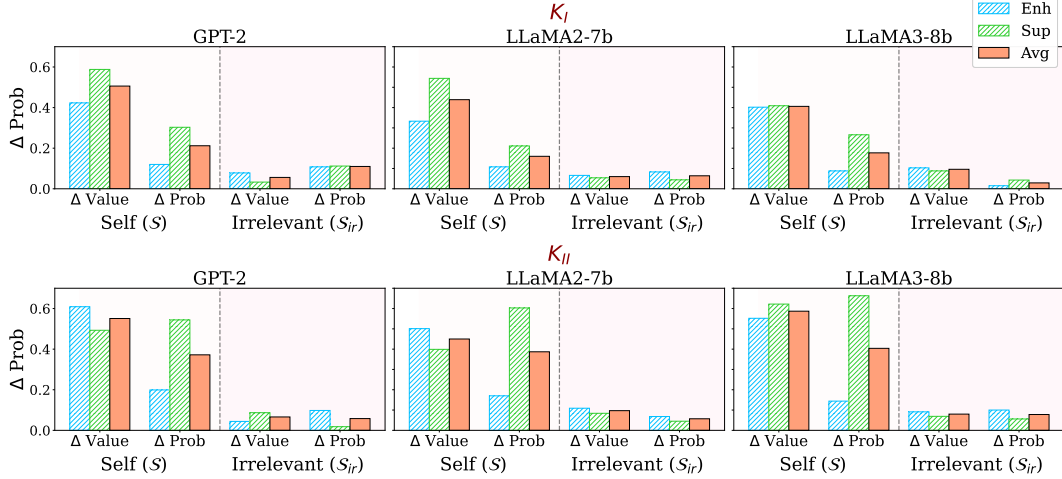


Figure 6: Results for the Dynamic KN Selection demonstration. “Self (S)” indicates knowledge synapses corresponding to the query itself, while “Irrelevant (S_{ir})” refers to those corresponding to an unrelated query. “ Δ Value” and “ Δ Prob” represent the rate of change in the average KN activation value and the PLMs’ answer probabilities, respectively. “Enh” and “Sup” refer to enhancement and suppression of the KS attention scores, respectively, with “Avg” representing their average.

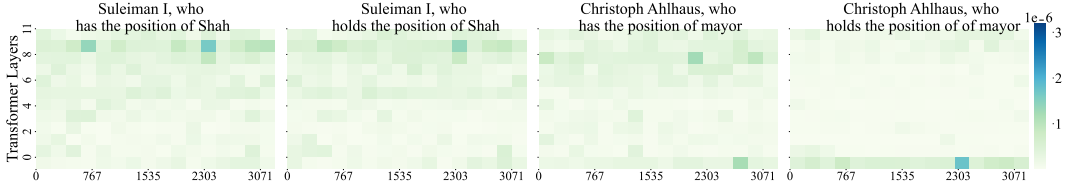


Figure 7: Heatmaps showing the neuron activation values, after suppressing knowledge synapses. The queries used here are the same as those in Figure 1. The dark areas in Figure 1 appear lighter here, indicating a decrease in the activation value of KNs. For the enhanced case, see Figure 10 in A.3.

Figure 5 illustrates the distributions of \mathcal{P} . The high values of \mathcal{P} suggest that the attention module tends to focus on specific tokens related to the dynamic context of the query. This observation leads us to propose the Dynamic KN Selection hypothesis, which posits that the attention module is not only “related” to the context but actively selects relevant KNs for a given query.

3.2.2 Demonstration of Dynamic KN Selection

Methods To prove the Dynamic KN Selection hypothesis, we either suppress or enhance attention scores related or unrelated to the query. Notably, attention score matrices resemble KN activation value matrices, differing only in an additional dimension for attention heads. Thus, similar to the definition of KNs, we identify column vectors with high attention scores. Drawing inspiration from cognitive science [8, 13, 17, 20, 30], we refer to these vectors as *Knowledge Synapses* (KSs), denoted as \mathcal{S} . Given a query with its answer, the KSs are defined as:

$$\tau = \alpha \cdot \frac{1}{L \cdot H} \sum_{l=1}^L \sum_{h=1}^H \sum_{r=1}^R \sum_{c=1}^C A_{(l,h)}^{(r,c)} \quad (5)$$

$$\mathcal{S} = \left\{ (c, l, h) \mid \sum_{r=1}^R A_{(l,h)}^{(r,c)} > \tau, \forall l \in \{1, \dots, L\}, h \in \{1, \dots, H\}, c \in \{1, \dots, C\} \right\} \quad (6)$$

where τ is the dynamic threshold, α is a scaling factor, and A is the attention score matrix. L and H represent the number of layers and heads of the attention module, respectively, while R and C are the rows and columns of A . l , h , r , c are the corresponding indices. After localizing \mathcal{S} , we enhance or

Table 3: Results of Consistency-Aware KN Modification. The metrics and settings are consistent with Table 2.

| Method | Erasure | | | | | | | | | | | | | | |
|-----------------------------------|----------------------|------|------|-------------|--------------|-----------|------|------|-------------|--------------|-----------|------|------|-------------|--------------|
| | GPT-2 | | | | | LLaMA2-7b | | | | | LLaMA3-8b | | | | |
| | Rel | Gen | Loc | Avg | ΔPPL | Rel | Gen | Loc | Avg | ΔPPL | Rel | Gen | Loc | Avg | ΔPPL |
| $K_I(\mathcal{N}_i)$ | 0.55 | 0.47 | 0.93 | 0.65 | 0.02 | 0.33 | 0.34 | 0.79 | 0.49 | 0.01 | 0.28 | 0.30 | 0.83 | 0.47 | 0.04 |
| $K_I(\mathcal{N}_g)$ | 0.58 | 0.55 | 0.90 | 0.68 | 0.12 | 0.30 | 0.55 | 0.70 | 0.52 | 0.08 | 0.30 | 0.35 | 0.80 | 0.48 | 0.18 |
| K_I (Ours) | 0.56 | 0.50 | 0.90 | 0.65 | 0.03 | 0.32 | 0.44 | 0.88 | 0.55 | 0.03 | 0.30 | 0.33 | 0.80 | 0.48 | 0.02 |
| $K_{II}(\mathcal{N}_i)$ | 0.50 | 0.09 | 0.97 | 0.52 | 0.06 | 0.36 | 0.11 | 0.80 | 0.42 | 0.03 | 0.34 | 0.04 | 0.90 | 0.43 | 0.05 |
| $K_{II}(\mathcal{N}_g)$ | 0.65 | 0.60 | 0.70 | 0.65 | 2.02 | 0.44 | 0.45 | 0.52 | 0.47 | 1.50 | 0.36 | 0.40 | 0.50 | 0.42 | 1.05 |
| K_{II} (Ours) | 0.55 | 0.40 | 0.90 | 0.62 | 0.10 | 0.35 | 0.35 | 0.77 | 0.49 | 0.06 | 0.34 | 0.30 | 0.88 | 0.51 | 0.09 |
| Update | | | | | | | | | | | | | | | |
| Method | GPT-2 | | | | | LLaMA2-7b | | | | | LLaMA3-8b | | | | |
| | Rel | Gen | Loc | Avg | ΔPPL | Rel | Gen | Loc | Avg | ΔPPL | Rel | Gen | Loc | Avg | ΔPPL |
| | $K_I(\mathcal{N}_i)$ | 0.53 | 0.40 | 0.99 | 0.64 | 0.04 | 0.30 | 0.39 | 0.89 | 0.53 | 0.03 | 0.30 | 0.29 | 0.79 | 0.46 |
| $K_I(\mathcal{N}_g)$ | 0.56 | 0.48 | 0.88 | 0.64 | 0.13 | 0.32 | 0.59 | 0.82 | 0.68 | 0.10 | 0.44 | 0.41 | 0.74 | 0.53 | 0.22 |
| K_I (Ours) | 0.55 | 0.44 | 0.98 | 0.66 | 0.14 | 0.30 | 0.50 | 0.88 | 0.56 | 0.10 | 0.35 | 0.33 | 0.70 | 0.46 | 0.10 |
| $K_{II}(\mathcal{N}_i)$ | 0.44 | 0.11 | 0.96 | 0.50 | 0.09 | 0.39 | 0.07 | 0.80 | 0.42 | 0.08 | 0.29 | 0.08 | 0.86 | 0.41 | 0.08 |
| $K_{II}(\mathcal{N}_g)$ | 0.54 | 0.55 | 0.74 | 0.61 | 1.88 | 0.40 | 0.43 | 0.62 | 0.48 | 1.16 | 0.29 | 0.33 | 0.66 | 0.43 | 0.93 |
| K_{II} (Ours) | 0.45 | 0.45 | 0.88 | 0.59 | 0.20 | 0.40 | 0.38 | 0.75 | 0.51 | 0.12 | 0.29 | 0.29 | 0.80 | 0.46 | 0.14 |

suppress the attention scores at these positions (i.e., KS attention scores) to study their effects. As a comparison, we randomly select knowledge synapses \mathcal{S}_{ir} corresponding to an irrelevant fact and perform the same operations.

Evaluation Metrics First, we assess the impact of manipulating knowledge synapses on the activation values of KNs. We calculate the rates of increase and decrease in the average KN activation values ($\overline{\text{Value}}$) before (b) and after (a) KS manipulation: $\Delta \text{Value} = \pm \frac{\overline{\text{Value}_a} - \overline{\text{Value}_b}}{\overline{\text{Value}_b}}$. Second, we compute the change in the PLMs' answer prediction probability (ΔProb). For ease of comparison, we average the results for suppression and enhancement in both settings.

Findings Figure 7 shows a case, and Figure 6 presents the overall results that establish the Dynamic KN Selection of the QL assumption. (1) Manipulating “Self(\mathcal{S})”, the attention scores related to the query, leads to corresponding changes in both KN activation value and the PLMs' answer probability. In contrast, manipulating “ \mathcal{S}_{ir} ” has a smaller effect, confirming that the changes are indeed caused by manipulating \mathcal{S} . (2) Figure 7 shows that suppressing KSs reduces KN activation values, creating confusion between KNs and other neurons. This makes it difficult for the attention module to select KNs and provide correct answers. Points (1) and (2) collectively demonstrate that attention module contributes to the selection of KNs, i.e., Dynamic KN Selection is established. (3) Furthermore, compared to K_I , K_{II} relies more on the attention module. As shown in Figure 6, manipulating the KSs has a larger impact on both ΔValue and ΔProb for K_{II} than for K_I .

3.3 Application of Query Localization Assumption: Consistency-Aware KN Modification

Experimental Setups Inspired by Query-KN Mapping hypothesis of the QL assumption, we propose a new approach to KN selection that improves knowledge modification methods. By incorporating KN consistency, we introduce the **Consistency-Aware Score (CAS)** metric, which penalizes low consistency and rewards high activation values. Given a fact with k queries, the CAS for the p -th neuron in the l -th MLP is defined as:

$$CAS_{(l,p)} = \beta_1 \mu_{lp} - \beta_2 \sigma_{lp}, \quad \text{where } \mu_{lp} = \frac{1}{k} \sum_{i=1}^k as_{lp}^{(i)}, \quad \sigma_{lp} = \sqrt{\frac{1}{k} \sum_{i=1}^k (as_{lp}^{(i)} - \mu_{lp})^2} \quad (7)$$

where β_1 and β_2 are hyperparameters, μ_{lp} and σ_{lp} represent the mean and variance, and $as_{lp}^{(i)}$ is the activation score at position (l, p) for q_i . Then, using thresholding techniques, we identify positions with high CAS values as the KNs to be edited and conduct experiments similar to those in §2.2.

Findings Table 3 presents the results, from which we conclude: (1) Our method exhibits superior and more balanced performance, particularly for K_{II} . For K_{II} , the “Avg” values of $K_{II}(\text{Ours})$ are notably higher than those of $K_{II}(\mathcal{N}_i)$, especially in terms of generalization. Simultaneously, it surpasses or closely matches the “Avg” values of $K_{II}(\mathcal{N}_g)$, especially in locality. Furthermore, the increase in PPL is much lower than that of $K_{II}(\mathcal{N}_g)$ and comparable to $K_{II}(\mathcal{N}_i)$, suggesting the small impact on the model’s general capabilities. (2) Our method is also shown to be effective for K_I . The performance of $K_I(\text{Ours})$ is comparable to both $K_I(\mathcal{N}_i)$ and $K_I(\mathcal{N}_g)$. This indicates that even facts adhering to the KL assumption can be effectively analyzed using the QL assumption, further illustrating the limitations of the KL assumption and showing that it is merely a simplification of the QL assumption.

4 Related Work

LLMs store extensive factual knowledge [27], prompting numerous studies to investigate the mechanisms behind their storage and expression. Geva et al. [11] propose that MLP modules simulate key-value memories to store information, and Dai et al. [7] propose the concept of knowledge neurons (KNs), suggesting that these MLP modules can store “knowledge”. The success of KN-inspired model editing methods [7, 22, 23] further supports the plausibility of the KN thesis. Additionally, the integrated gradients (IG) method [37] has proven suitable for knowledge localization [21], leading to further refinements such as Sequential IG, Discretized IG and the Architecture adapted Multilingual IG [4, 10, 25, 35, 36]. Further investigations reveal that some KNs exhibit cross-lingual features [4, 29, 42, 46], while others display language-specific characteristics [18, 38, 47]. Some KNs also show degeneracy, with multiple neurons redundantly encoding the same factual knowledge [5]. These studies collectively advance the KN thesis. Beyond MLP modules, some studies incorporate attention modules [40] into factual knowledge research. They find that attention modules play a role in the PLMs’ internal information flow, aiding in factual knowledge extraction [12]. Moreover, attention modules can facilitate in-context learning [32] and relate to token expression [22].

However, the KN thesis has its limitations. Niu et al. [26] argue that it oversimplifies the real situation, while Hase et al. [14] suggest that the location of knowledge localization may not align with the location of greatest impact on knowledge expression. Additionally, the research has found that neurons can be further decomposed into features [34], and the activation of a single neuron can have different meanings in different contexts [33]. Limitations in KN-inspired knowledge editing methods have also been identified [6, 15, 16, 19, 28, 41, 43, 45]. These model editing methods may fail to edit successfully or impair the PLMs’ general capabilities, indirectly suggesting issues with the KN thesis. However, previous works mainly observe problems with the KN thesis and identify phenomena through experiments, without deeply analyzing their causes or providing effective solutions. Our work not only analyzes the inherent issues of the KN thesis but also proposes solutions.

5 Conclusion and Future Work

This paper investigates the Knowledge Localization (KL) assumption of the knowledge neuron (KN) thesis, which posits that a piece of factual knowledge can be localized to several knowledge neurons. We re-examine this assumption and confirm that much factual knowledge does not conform to it. Furthermore, we propose and validate the Query Localization (QL) assumption, which includes two aspects: Query-KN Mapping and Dynamic KN Selection. Extensive experiments validate the QL assumption and suggest that the KL assumption is essentially a simplification of the QL assumption. Future work could delve into the reasons behind the existence of K_{II} and explore how to further utilize the QL assumption, along with the properties of K_{II} , to improve the model editing method.

References

- [1] Otsu’s method - wikipedia. URL https://en.wikipedia.org/wiki/Otsu%27s_method.
- [2] Welch’s t-test - wikipedia. URL https://en.wikipedia.org/wiki/Welch%27s_t-test.
- [3] Meta AI. Introducing meta llama 3: The most capable openly available llm to date. URL <https://ai.meta.com/blog/meta-llama-3/>.
- [4] Yuheng Chen, Pengfei Cao, Yubo Chen, Kang Liu, and Jun Zhao. Journey to the center of the knowledge neurons: Discoveries of language-independent knowledge neurons and degenerate knowledge neurons. In *Proceedings of the AAAI Conference on Artificial Intelligence*, volume 38, pages 17817–17825, 2024. URL <https://ojs.aaai.org/index.php/AAAI/article/view/29735>.
- [5] Yuheng Chen, Pengfei Cao, Yubo Chen, Yining Wang, Shengping Liu, Kang Liu, and Jun Zhao. The da vinci code of large pre-trained language models: Deciphering degenerate knowledge neurons, 2024. URL <https://arxiv.org/abs/2402.13731>.
- [6] Roi Cohen, Eden Biran, Ori Yoran, Amir Globerson, and Mor Geva. Evaluating the ripple effects of knowledge editing in language models. *ArXiv preprint*, abs/2307.12976, 2023. URL <https://arxiv.org/abs/2307.12976>.
- [7] Damai Dai, Li Dong, Yaru Hao, Zhifang Sui, Baobao Chang, and Furu Wei. Knowledge neurons in pretrained transformers. In *Proceedings of the 60th Annual Meeting of the Association for Computational Linguistics (Volume 1: Long Papers)*, pages 8493–8502, Dublin, Ireland, 2022. Association for Computational Linguistics. doi: 10.18653/v1/2022.acl-long.581. URL <https://aclanthology.org/2022.acl-long.581>.
- [8] Matthew B Dalva, Andrew C McClelland, and Matthew S Kayser. Cell adhesion molecules: signalling functions at the synapse. *Nature Reviews Neuroscience*, 8(3):206–220, 2007. URL <https://www.nature.com/articles/nrn2075>.
- [9] Yanai Elazar, Nora Kassner, Shauli Ravfogel, Abhilasha Ravichander, Eduard Hovy, Hinrich Schütze, and Yoav Goldberg. Measuring and improving consistency in pretrained language models. *Transactions of the Association for Computational Linguistics*, 9:1012–1031, 2021. doi: 10.1162/tacl_a_00410. URL <https://aclanthology.org/2021.tacl-1.60>.
- [10] Joseph Enguehard. Sequential integrated gradients: a simple but effective method for explaining language models. *ArXiv preprint*, abs/2305.15853, 2023. URL <https://arxiv.org/abs/2305.15853>.
- [11] Mor Geva, Roei Schuster, Jonathan Berant, and Omer Levy. Transformer feed-forward layers are key-value memories. In *Proceedings of the 2021 Conference on Empirical Methods in Natural Language Processing*, pages 5484–5495, Online and Punta Cana, Dominican Republic, 2021. Association for Computational Linguistics. doi: 10.18653/v1/2021.emnlp-main.446. URL <https://aclanthology.org/2021.emnlp-main.446>.
- [12] Mor Geva, Jasmijn Bastings, Katja Filippova, and Amir Globerson. Dissecting recall of factual associations in auto-regressive language models. In *The 2023 Conference on Empirical Methods in Natural Language Processing*, 2023. URL <https://openreview.net/forum?id=F1G7y94K02>.
- [13] Padinhare Cholakkal Harikesh, Chi-Yuan Yang, Deyu Tu, Jennifer Y Gerasimov, Abdul Manan Dar, Adam Armada-Moreira, Matteo Massetti, Renee Kroon, David Bliman, Roger Ols-son, et al. Organic electrochemical neurons and synapses with ion mediated spiking. *Nature communications*, 13(1):901, 2022. URL <https://www.nature.com/articles/s41467-022-28483-6#citeas>.
- [14] Peter Hase, Mohit Bansal, Been Kim, and Asma Ghandeharioun. Does localization inform editing? surprising differences in causality-based localization vs. knowledge editing in language models. In *Thirty-seventh Conference on Neural Information Processing Systems*, 2023. URL <https://openreview.net/forum?id=ElDbU1Ztbd>.

[15] Jason Hoelscher-Obermaier, Julia Persson, Esben Kran, Ioannis Konstas, and Fazl Barez. Detecting edit failures in large language models: An improved specificity benchmark. In Anna Rogers, Jordan Boyd-Graber, and Naoaki Okazaki, editors, *Findings of the Association for Computational Linguistics: ACL 2023*, pages 11548–11559, Toronto, Canada, 2023. Association for Computational Linguistics. doi: 10.18653/v1/2023.findings-acl.733. URL <https://aclanthology.org/2023.findings-acl.733>.

[16] Wenyue Hua, Jiang Guo, Mingwen Dong, Henghui Zhu, Patrick Ng, and Zhiguo Wang. Propagation and pitfalls: Reasoning-based assessment of knowledge editing through counterfactual tasks. *arXiv preprint arXiv:2401.17585*, 2024. URL <https://arxiv.org/abs/2401.17585>.

[17] Seungjoon Kim, Hyeyonho Kim, and Ji Won Um. Synapse development organized by neuronal activity-regulated immediate-early genes. *Experimental & molecular medicine*, 50(4):1–7, 2018. URL <https://www.nature.com/articles/nrn2075>.

[18] Takeshi Kojima, Itsuki Okimura, Yusuke Iwasawa, Hitomi Yanaka, and Yutaka Matsuo. On the multilingual ability of decoder-based pre-trained language models: Finding and controlling language-specific neurons, 2024. URL <https://arxiv.org/abs/2404.02431>.

[19] Zhoubo Li, Ningyu Zhang, Yunzhi Yao, Mengru Wang, Xi Chen, and Huajun Chen. Unveiling the pitfalls of knowledge editing for large language models. In *The Twelfth International Conference on Learning Representations*, 2024. URL <https://openreview.net/forum?id=fNktD3ib16>.

[20] John Lisman, Katherine Cooper, Megha Sehgal, and Alcino J Silva. Memory formation depends on both synapse-specific modifications of synaptic strength and cell-specific increases in excitability. *Nature neuroscience*, 21(3):309–314, 2018. URL <https://www.nature.com/articles/s41593-018-0076-6#citeas>.

[21] Daniel Lundström, Tianjian Huang, and Meisam Razaviyayn. A rigorous study of integrated gradients method and extensions to internal neuron attributions. In Kamalika Chaudhuri, Stefanie Jegelka, Le Song, Csaba Szepesvári, Gang Niu, and Sivan Sabato, editors, *International Conference on Machine Learning, ICML 2022, 17-23 July 2022, Baltimore, Maryland, USA*, volume 162 of *Proceedings of Machine Learning Research*, pages 14485–14508. PMLR, 2022. URL <https://proceedings.mlr.press/v162/1lundstrom22a.html>.

[22] Kevin Meng, David Bau, Alex J Andonian, and Yonatan Belinkov. Locating and editing factual associations in GPT. In Alice H. Oh, Alekh Agarwal, Danielle Belgrave, and Kyunghyun Cho, editors, *Advances in Neural Information Processing Systems*, 2022. URL <https://openreview.net/forum?id=-h6WAS6eE4>.

[23] Kevin Meng, Arnab Sen Sharma, Alex J Andonian, Yonatan Belinkov, and David Bau. Mass-editing memory in a transformer. In *The Eleventh International Conference on Learning Representations*, 2023. URL <https://openreview.net/forum?id=MkbcAHTYgyS>.

[24] Stephen Merity, Caiming Xiong, James Bradbury, and Richard Socher. Pointer sentinel mixture models. In *5th International Conference on Learning Representations, ICLR 2017, Toulon, France, April 24-26, 2017, Conference Track Proceedings*. OpenReview.net, 2017. URL <https://openreview.net/forum?id=Byj72udxe>.

[25] Vivek Miglani, Narine Kokhlikyan, Bilal Alsallakh, Miguel Martin, and Orion Reblitz-Richardson. Investigating saturation effects in integrated gradients. *ArXiv preprint, abs/2010.12697*, 2020. URL <https://arxiv.org/abs/2010.12697>.

[26] Jingcheng Niu, Andrew Liu, Zining Zhu, and Gerald Penn. What does the knowledge neuron thesis have to do with knowledge? In *The Twelfth International Conference on Learning Representations*, 2024. URL <https://openreview.net/forum?id=2HJRwwbV3G>.

[27] Fabio Petroni, Tim Rocktäschel, Sebastian Riedel, Patrick Lewis, Anton Bakhtin, Yuxiang Wu, and Alexander Miller. Language models as knowledge bases? In *Proceedings of the 2019 Conference on Empirical Methods in Natural Language Processing and the 9th International Joint Conference on Natural Language Processing (EMNLP-IJCNLP)*, pages 2463–2473, Hong Kong, China, 2019. Association for Computational Linguistics. doi: 10.18653/v1/D19-1250. URL <https://aclanthology.org/D19-1250>.

[28] Yuval Pinter and Michael Elhadad. Emptying the ocean with a spoon: Should we edit models? In *The 2023 Conference on Empirical Methods in Natural Language Processing*, 2023. URL <https://openreview.net/forum?id=2wFVkTDG0Z>.

[29] Jirui Qi, Raquel Fernández, and Arianna Bisazza. Cross-lingual consistency of factual knowledge in multilingual language models. In *The 2023 Conference on Empirical Methods in Natural Language Processing*, 2023. URL <https://openreview.net/forum?id=MLKLYoXypN>.

[30] Ithai Rabinowitch, Daniel A Colón-Ramos, and Michael Krieg. Understanding neural circuit function through synaptic engineering. *Nature Reviews Neuroscience*, pages 1–9, 2024. URL <https://www.nature.com/articles/s41583-023-00777-8>.

[31] Alec Radford, Jeffrey Wu, Rewon Child, David Luan, Dario Amodei, Ilya Sutskever, et al. Language models are unsupervised multitask learners. *OpenAI blog*, 1(8):9, 2019. URL https://d4mucfpksywv.cloudfront.net/better-language-models/language_models_are_unsupervised_multitask_learners.pdf.

[32] Jie Ren, Qipeng Guo, Hang Yan, Dongrui Liu, Xipeng Qiu, and Dahua Lin. Identifying semantic induction heads to understand in-context learning. *ArXiv preprint*, abs/2402.13055, 2024. URL <https://arxiv.org/abs/2402.13055>.

[33] Claude AI research blog. Distributed representations: Composition & superposition. *Transformer Circuits Thread*, . URL <https://transformer-circuits.pub/2023/superposition-composition/index.html>.

[34] Claude AI research blog. Towards monosemanticity: Decomposing language models with dictionary learning. *Transformer Circuits Thread*, . URL <https://transformer-circuits.pub/2023/monosemantic-features>.

[35] Soumya Sanyal and Xiang Ren. Discretized integrated gradients for explaining language models. In *Proceedings of the 2021 Conference on Empirical Methods in Natural Language Processing*, pages 10285–10299, Online and Punta Cana, Dominican Republic, 2021. Association for Computational Linguistics. doi: 10.18653/v1/2021.emnlp-main.805. URL <https://aclanthology.org/2021.emnlp-main.805>.

[36] Sandipan Sikdar, Parantapa Bhattacharya, and Kieran Heese. Integrated directional gradients: Feature interaction attribution for neural NLP models. In *Proceedings of the 59th Annual Meeting of the Association for Computational Linguistics and the 11th International Joint Conference on Natural Language Processing (Volume 1: Long Papers)*, pages 865–878, Online, 2021. Association for Computational Linguistics. doi: 10.18653/v1/2021.acl-long.71. URL <https://aclanthology.org/2021.acl-long.71>.

[37] Mukund Sundararajan, Ankur Taly, and Qiqi Yan. Axiomatic attribution for deep networks. In Doina Precup and Yee Whye Teh, editors, *Proceedings of the 34th International Conference on Machine Learning, ICML 2017, Sydney, NSW, Australia, 6-11 August 2017*, volume 70 of *Proceedings of Machine Learning Research*, pages 3319–3328. PMLR, 2017. URL <http://proceedings.mlr.press/v70/sundararajan17a.html>.

[38] Tianyi Tang, Wenyang Luo, Haoyang Huang, Dongdong Zhang, Xiaolei Wang, Xin Zhao, Furu Wei, and Ji-Rong Wen. Language-specific neurons: The key to multilingual capabilities in large language models. *ArXiv preprint*, abs/2402.16438, 2024. URL <https://arxiv.org/abs/2402.16438>.

[39] Hugo Touvron, Louis Martin, Kevin Stone, Peter Albert, Amjad Almahairi, Yasmine Babaei, Nikolay Bashlykov, Soumya Batra, Prajjwal Bhargava, Shruti Bhosale, Dan Bikel, Lukas Blecher, Cristian Canton Ferrer, Moya Chen, Guillem Cucurull, David Esiobu, Jude Fernandes, Jeremy Fu, Wenyin Fu, Brian Fuller, Cynthia Gao, Vedanuj Goswami, Naman Goyal, Anthony Hartshorn, Saghaf Hosseini, Rui Hou, Hakan Inan, Marcin Kardas, Viktor Kerkez, Madian Khabsa, Isabel Kloumann, Artem Korenev, Punit Singh Koura, Marie-Anne Lachaux, Thibaut Lavril, Jenya Lee, Diana Liskovich, Yinghai Lu, Yuning Mao, Xavier Martinet, Todor Mihaylov, Pushkar Mishra, Igor Molybog, Yixin Nie, Andrew Poulton, Jeremy Reizenstein, Rashi Rungta, Kalyan Saladi, Alan Schelten, Ruan Silva, Eric Michael Smith, Ranjan Subramanian, Xiaojing Ellen Tan, Binh Tang, Ross Taylor, Adina Williams, Jian Xiang Kuan, Puxin Xu, Zheng

Yan, Iliyan Zarov, Yuchen Zhang, Angela Fan, Melanie Kambadur, Sharan Narang, Aurelien Rodriguez, Robert Stojnic, Sergey Edunov, and Thomas Scialom. Llama 2: Open foundation and fine-tuned chat models, 2023. URL <https://arxiv.org/abs/2307.09288>.

[40] Ashish Vaswani, Noam Shazeer, Niki Parmar, Jakob Uszkoreit, Llion Jones, Aidan N. Gomez, Łukasz Kaiser, and Illia Polosukhin. Attention is all you need. In Isabelle Guyon, Ulrike von Luxburg, Samy Bengio, Hanna M. Wallach, Rob Fergus, S. V. N. Vishwanathan, and Roman Garnett, editors, *Advances in Neural Information Processing Systems 30: Annual Conference on Neural Information Processing Systems 2017, December 4-9, 2017, Long Beach, CA, USA*, pages 5998–6008, 2017. URL <https://proceedings.neurips.cc/paper/2017/hash/3f5ee243547dee91fb053c1c4a845aa-Abstract.html>.

[41] Jianchen Wang, Zhouhong Gu, Zhuozhi Xiong, Hongwei Feng, and Yanghua Xiao. The missing piece in model editing: A deep dive into the hidden damage brought by model editing. *ArXiv preprint*, abs/2403.07825, 2024. URL <https://arxiv.org/abs/2403.07825>.

[42] Zhihui Xie, Handong Zhao, Tong Yu, and Shuai Li. Discovering low-rank subspaces for language-agnostic multilingual representations. In *Proceedings of the 2022 Conference on Empirical Methods in Natural Language Processing*, pages 5617–5633, Abu Dhabi, United Arab Emirates, 2022. Association for Computational Linguistics. URL <https://aclanthology.org/2022.emnlp-main.379>.

[43] Yunzhi Yao, Peng Wang, Bozhong Tian, Siyuan Cheng, Zhoubo Li, Shumin Deng, Huajun Chen, and Ningyu Zhang. Editing large language models: Problems, methods, and opportunities. In Houda Bouamor, Juan Pino, and Kalika Bali, editors, *Proceedings of the 2023 Conference on Empirical Methods in Natural Language Processing*, pages 10222–10240, Singapore, 2023. Association for Computational Linguistics. doi: 10.18653/v1/2023.emnlp-main.632. URL <https://aclanthology.org/2023.emnlp-main.632>.

[44] Zhihao Zhang, Jun Zhao, Qi Zhang, Tao Gui, and Xuanjing Huang. Unveiling linguistic regions in large language models. *arXiv preprint arXiv:2402.14700*, 2024.

[45] Jun Zhao, Zhihao Zhang, Yide Ma, Qi Zhang, Tao Gui, Luhui Gao, and Xuanjing Huang. Unveiling a core linguistic region in large language models, 2023.

[46] Xin Zhao, Naoki Yoshinaga, and Daisuke Oba. Tracing the roots of facts in multilingual language models: Independent, shared, and transferred knowledge, 2024. URL <https://arxiv.org/abs/2403.05189>.

[47] Yiran Zhao, Wenxuan Zhang, Guizhen Chen, Kenji Kawaguchi, and Lidong Bing. How do large language models handle multilingualism? *ArXiv preprint*, abs/2402.18815, 2024. URL <https://arxiv.org/abs/2402.18815>.

A Appendix

A.1 Specific Experimental Settings

Hardware specification and environment. We ran our experiments on the machine equipped with the following specifications:

- CPU: Intel(R) Xeon(R) CPU E5-2680 v4 @ 2.40GHz, Total CPUs: 56
- GPU:
 - NVIDIA GeForce RTX 3090 × 20. The Standard Memory Config is 24 GB GDDR6X.
 - NVIDIA A100 80GB PCIe × 4. The GPU Memory is 80GB HBM2e.
- Software:
 - Python Version: 3.10.10
 - PyTorch Version: 2.0.0+cu117

Table 4: This table corresponds to Table 1 and lists the thresholds for each experimental setting.

| GPT2 | | | |
|-----------|----------------|----------------|-----------------|
| T | Dai et al. [7] | Enguehard [10] | Chen et al. [4] |
| Static | 0.1 | 0.1 | 0.1 |
| Otsu | 0.146 | 0.150 | 0.148 |
| LLaMA2-7b | | | |
| T | Dai et al. [7] | Enguehard [10] | Chen et al. [4] |
| Static | 0.1 | 0.1 | 0.1 |
| Otsu | 0.170 | 0.169 | 0.170 |
| LLaMA3-8b | | | |
| T | Dai et al. [7] | Enguehard [10] | Chen et al. [4] |
| Static | 0.1 | 0.1 | 0.1 |
| Otsu | 0.080 | 0.082 | 0.081 |

In the experiments, the main computational expense was associated with acquiring knowledge neurons since the method for knowledge localization computes the activation values of all neurons. For GPT-2, LLaMA2-7b, and LLaMA3-8b, the time required to acquire KNs once was approximately: 20 seconds, 5 minutes, and 5 minutes, respectively. As we conducted our experiments using multi-GPU distributed processing, the total time spent was about 26 days. The computational expense for the other experiments was not significant, and they could be completed within 10 days. Due to the lengthy computation times, we tested the code and results by selecting one datum from each relation, thus the test dataset comprised only 36 data points. We did conduct some erroneous experiments, but the run-time costs for these were negligible due to the small size of the test dataset. We recommend that readers adopt a similar approach for testing their code.

Experimental Hyperparameters of Consistency Analysis We provide the thresholds used for each setting in Table 4, corresponding to Table 1. The Otsu threshold is calculated separately based on each batch of data, thus each is different. The static threshold is set by us, thus it is the same.

Experimental Hyperparameters of KN Modification In Equation 2, we set $\lambda_1 = \lambda_2 = 2$.

Experimental Hyperparameters of Obtaining Knowledge Synapses In Equations 5 and 6, the scaling factor τ is the same for all three PLMs, with $\tau = 0.3$.

Experimental Hyperparameters of Consistency-Aware KN Modification In Equation 7, we set $\beta_1 = 0.7$ and $\beta_2 = 0.3$. For the selection of threshold, we consider the dynamic threshold to find the maximum value of CAS, and neurons larger than 0.3 times are selected as KNs.

A.2 Experimental Dataset Introduction

In our experiments, we selected the ParaRel dataset [9], a high-quality resource of cloze-style query English paraphrases. It contains a total of 328 paraphrases for 38 relations. We further conducted a basic filtering, excluding 2 relations that had no paraphrases. Table 5 displays these relations and corresponding example data.

A.3 Supplementary Experimental Results

Supplementary Experimental Results of Consistency Analysis (§2.1) Figure 8 and Figure 9 show two violin plots. The experimental settings are exactly the same as Figure 3, but the knowledge positioning is different. Figure 8 and Figure 9 adopt the knowledge positioning methods proposed by Enguehard [10] and Chen et al. [4] respectively.

Table 5: Example data of the ParaRel dataset [9].

| Relation | Example data | |
|----------|--|--------------|
| | Example Query | Answer |
| P39 | Adrian IV has the position of | pope |
| P264 | Purple Hearts is represented by music label | Sunshine |
| P37 | The official language of Republic of Ingushetia is | Russian |
| P108 | Henry Swanzey works for | BBC |
| P131 | Heaton Park is located in | Manchester |
| P103 | The native language of Francis Ponge is | French |
| P176 | Fiat Grande Punto is produced by | Fiat |
| P30 | Somalia is located in | Africa |
| P178 | Gain Ground is developed by | Sega |
| P138 | International Day for Biological Diversity is named after | biodiversity |
| P47 | Ukraine shares border with | Poland |
| P17 | Media Development Authority is located in | Singapore |
| P413 | Joe Torre plays in [MASK] position. | catcher |
| P27 | Edward Wollstonecraft is [MASK] citizen. | Australia |
| P463 | Chuck Schuldiner is a member of | Death |
| P364 | The original language of NU.nl is | Dutch |
| P495 | The Creepshow was created in | Canada |
| P449 | Yes Minister was originally aired on | BBC |
| P20 | Margaret Cavendish, Duchess of Newcastle-upon-Tyne died in | England |
| P1376 | Rumbek is the capital of | Lakes |
| P1001 | Minister for Foreign Affairs is a legal term in | Australia |
| P361 | propellant is part of | cartridge |
| P36 | The capital of Flanders is | Brussels |
| P1303 | Ludovico Einaudi plays | piano |
| P530 | Brunei maintains diplomatic relations with | Australia |
| P19 | Lopo Soares de Albergaria was born in | Lisbon |
| P190 | Bratislava and [MASK] are twin cities. | Dublin |
| P740 | Shirehorses was founded in | Manchester |
| P136 | Frank Mantooth plays [MASK] music. | jazz |
| P127 | AVCHD is owned by | Sony |
| P1412 | Karl Bodmer used to communicate in | French |
| P407 | Zarez was written in | Croatian |
| P140 | Leo IX is affiliated with the [MASK] religion. | Christianity |
| P279 | quinquina is a subclass of | wine |
| P276 | Al-Rifa'i Mosque is located in | Cairo |
| P159 | The headquarter of Allied Command Transformation is in | Norfolk |
| P106 | Giuseppe Saracco is a [MASK] by profession. | politician |
| P101 | Aleksei N. Leontiev works in the field of | psychology |
| P937 | Joseph Chamberlain used to work in | London |

Supplementary Experimental Results of Heatmap of Neuron Activations (Figures 1 and 7)
 Figure 10 shows the neuron activation values under three conditions: 1. No manipulation of knowledge synapses, 2. Suppressing knowledge synapses, and 3. Enhancing knowledge synapses. The chosen queries remain consistent.

A.4 Knowledge Localization Methods

We have adopted three advanced knowledge localization methods, and the specific experimental settings remain consistent with the original author. Below we introduce their specific details.

Integrated Gradients [7] Dai et al. [7] propose the IG method. Given an input prompt x , the method defines the model output $P_x(\hat{w}_i^{(l)})$ as the probability of the correct answer predicted by a

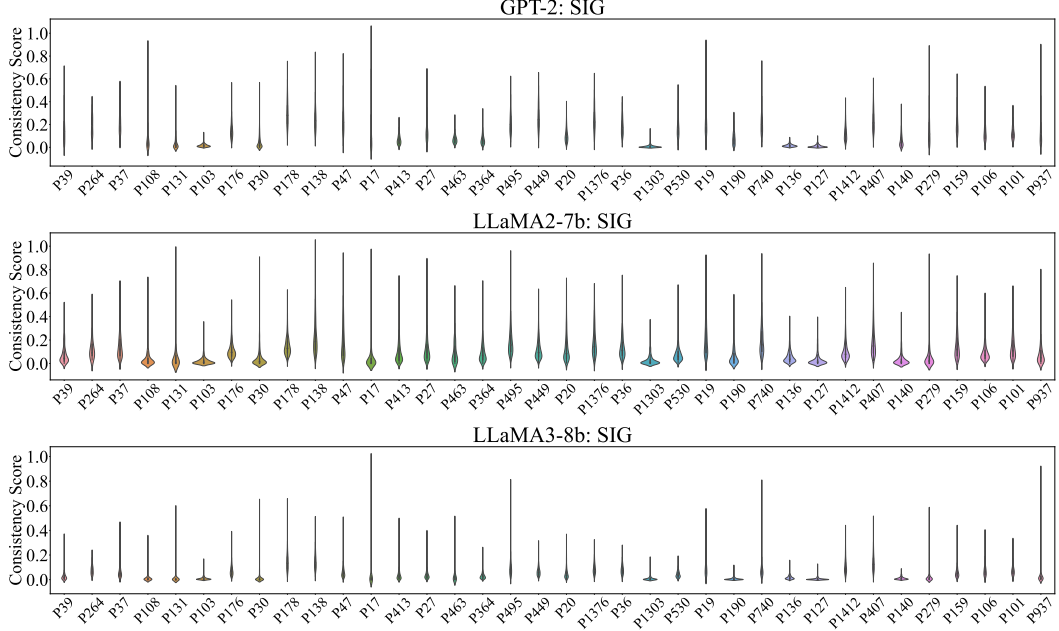


Figure 8: Violin Plot of Consistency Analysis. The experimental settings are exactly the same as Figure 3, but the knowledge positioning method used here is the method proposed by Enguehard [10].

pretrained model:

$$P_x(\hat{w}_i^{(l)}) = p(y^* | x, w_i^{(l)} = \hat{w}_i^{(l)}) \quad (8)$$

where y^* is the correct answer, $w_i^{(l)}$ is the i -th intermediate neuron in the l -th MLP, and $\hat{w}_i^{(l)}$ is a constant assigned to $w_i^{(l)}$.

To calculate the attribution score of a neuron $\text{Attr}(w_i^{(l)})$, they change $w_i^{(l)}$ gradually from 0 to its original value $\bar{w}_i^{(l)}$ and integrate the gradients to determine the impact of the neuron:

$$\text{Attr}(w_i^{(l)}) = \bar{w}_i^{(l)} \int_{\alpha=0}^1 \frac{\partial P_x(\alpha \bar{w}_i^{(l)})}{\partial w_i^{(l)}} d\alpha \quad (9)$$

where $\frac{\partial P_x(\alpha \bar{w}_i^{(l)})}{\partial w_i^{(l)}}$ is the gradient of the model output with respect to $w_i^{(l)}$. As α changes from 0 to 1, integrating the gradients allows the attribution score to accumulate the change in output probability caused by modifying $w_i^{(l)}$. If a neuron significantly influences factual expressions, its gradient will be more salient, leading to larger integrated values. Thus, the attribution score measures the contribution of a neuron $w_i^{(l)}$ to factual expression.

Calculating the continuous integral directly is challenging, thus they approximate it using a Riemann sum:

$$\tilde{\text{Attr}}(w_i^{(l)}) = \frac{\bar{w}_i^{(l)}}{m} \sum_{k=1}^m \frac{\partial P_x\left(\frac{k}{m} \bar{w}_i^{(l)}\right)}{\partial w_i^{(l)}} \quad (10)$$

where $m = 20$ is the number of approximation steps. With the attribution algorithm, they identify a coarse set of knowledge neurons by selecting those whose attribution scores exceed a predefined threshold.

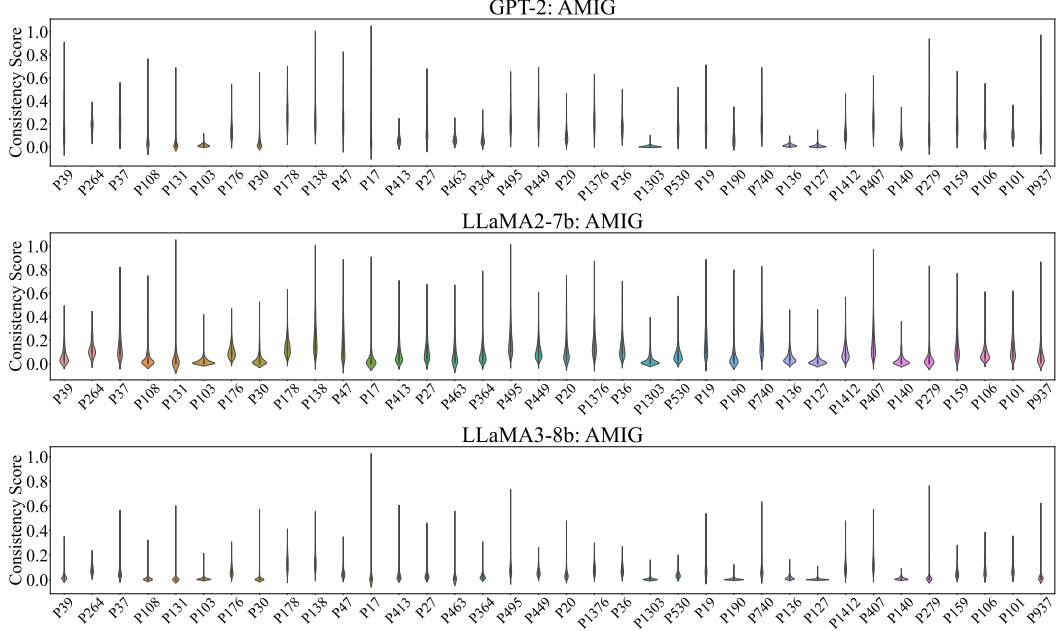


Figure 9: Violin Plot of Consistency Analysis. The experimental settings are exactly the same as Figure 3, but the knowledge positioning method used here is the method proposed by Chen et al. [4].

Sequential Integrated Gradients [10] Enguehard [10] propose the SIG method. A language model is defined as a function:

$$F(\mathbf{x}) : \mathbb{R}^{m \times n} \rightarrow \mathbb{R} \quad (11)$$

where \mathbf{x} is a sequence of m words, each represented by n features, typically derived from an embedding layer. The output of the function F is a single value, such as a sentiment score for a given sentence. \mathbf{x}_i denotes the i -th word of a sequence, and x_{ij} represents the j -th feature of the i -th word. For each word \mathbf{x}_i , a baseline $\bar{\mathbf{x}}^i$ is defined as the original sequence with \mathbf{x}_i replaced by a mask token:

$$\bar{\mathbf{x}}^i = (\mathbf{x}_1, \dots, \text{<mask>}, \dots, \mathbf{x}_m) \quad (12)$$

where the mask token replaces only the word of interest. If the model lacks a “mask” token (e.g., GPT-2), a “pad” token is used.

SIG calculates the attribution score for a word \mathbf{x}_i and feature j as:

$$\text{SIG}_{ij}(\mathbf{x}) := (x_{ij} - \bar{x}_{ij}) \times \int_0^1 \frac{\partial F(\bar{\mathbf{x}}^i + \alpha \times (\mathbf{x} - \bar{\mathbf{x}}^i))}{\partial x_{ij}} d\alpha \quad (13)$$

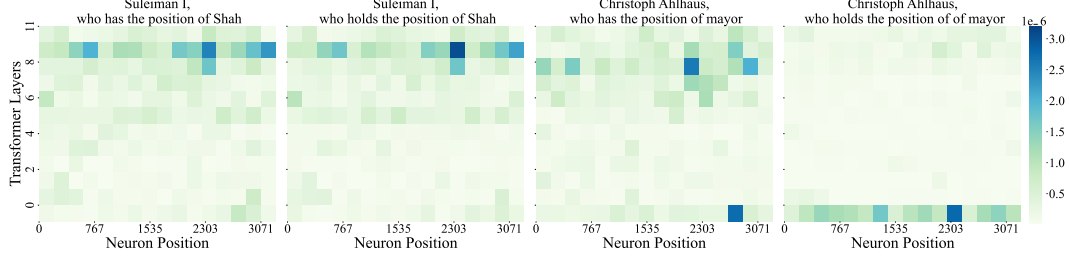
where the integral measures the gradient of F along the straight line between $\bar{\mathbf{x}}^i$ and \mathbf{x} . Similar to the original Integrated Gradients (IG) method, the integral is approximated using a Riemann sum. The integral is evaluated across a straight line path between the baseline $\bar{\mathbf{x}}^i$ and the original input \mathbf{x} . The total attribution score for a word \mathbf{x}_i is computed by summing across all features j and normalizing the result:

$$\text{SIG}_i(\mathbf{x}) := \frac{\sum_j \text{SIG}_{ij}}{\|\text{SIG}\|} \quad (14)$$

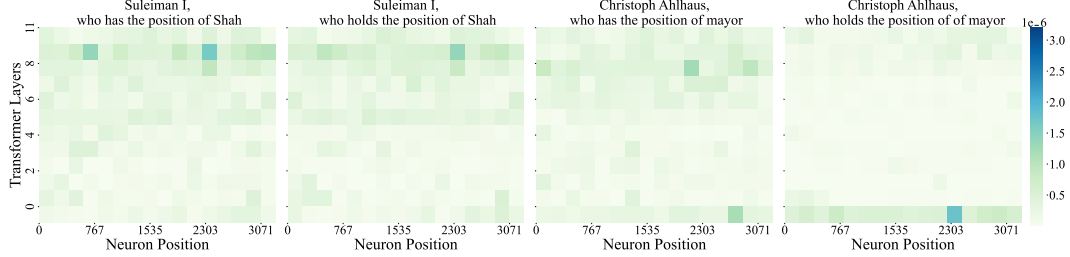
Architecture-adapted Multilingual Integrated Gradients [4] Chen et al. [4] propose the AMIG method. Given a query q , they define the probability of the correct answer predicted by a PLMs as follows:

$$F(\hat{w}_j^{(l)}) = p(y^* | q, w_j^{(l)} = \hat{w}_j^{(l)}) \quad (15)$$

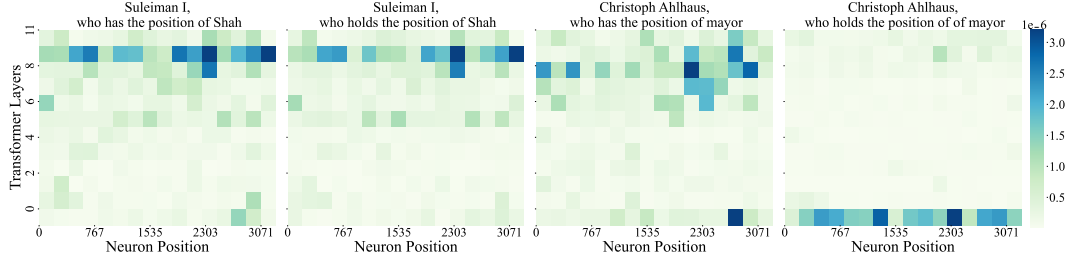
Here, y^* represents the correct answer, $w_j^{(l)}$ denotes the j -th neuron in the l -th layer, and $\hat{w}_j^{(l)}$ is the specific value assigned to $w_j^{(l)}$. To calculate the attribution score for each neuron, they employ the



(a) Does not manipulate knowledge synapses.



(b) Suppress the knowledge synapses.



(c) Enhance the knowledge synapses.

Figure 10: Heatmap of neuron activations. From top to bottom, the three images correspond to: (a). No manipulation of knowledge synapses, (b). Suppressing knowledge synapses, and (c). Enhancing knowledge synapses. The chosen queries remain consistent.

technique of integrated gradients. To compute the attribution score of a neuron $w_j^{(l)}$, they consider the following formulation:

$$\text{Attr}(w_j^{(l)}) = (\bar{w}_j^{(l)} - w_j'^{(l)}) \int_0^1 \frac{\partial F(w_j'^{(l)} + \alpha(\bar{w}_j^{(l)} - w_j'^{(l)}))}{\partial w_j^{(l)}} d\alpha \quad (16)$$

Here, $\bar{w}_j^{(l)}$ represents the actual value of $w_j^{(l)}$, $w_j'^{(l)}$ serves as the baseline vector for $w_j^{(l)}$. The term $\frac{\partial F(w_j'^{(l)} + \alpha(w_j^{(l)} - w_j'^{(l)}))}{\partial w_j^{(l)}}$ computes the gradient with respect to $w_j^{(l)}$. Next, they aim to obtain $w_j'^{(l)}$.

Starting from the sentence q , they acquire a baseline sentence and then encode this sentence as a vector. Let the baseline sentence corresponding to q_i be q'_i , and q'_i consists of m words, maintaining a length consistent with q , denoted as $q'_i = (q'_{i1} \dots q'_{ik} \dots q'_{im})$. Since they are using auto-regressive models, according to Chen et al. [4], $q'_{ik} = \langle \text{eos} \rangle$, where $\langle \text{eos} \rangle$ represents “end of sequence” in auto-regressive models. The attribution score $\text{Attr}_i(w_j^{(l)})$ for each neuron, given the input q_i , can be determined using Equation (16). For the computation of the integral, the Riemann approximation method is employed:

$$\text{Attr}_i(w_j^{(l)}) \approx \frac{\bar{w}_j^{(l)}}{N} \sum_{k=1}^N \frac{\partial F(w_j'^{(l)} + \frac{k}{N} \times (\bar{w}_j^{(l)} - w_j'^{(l)}))}{\partial w_j^{(l)}} \quad (17)$$

where N is the number of approximation steps. Then, the attribution scores for each word q_i are aggregated and subsequently normalized:

$$Attr(w_j^l) = \frac{\sum_{i=1}^m Attr_i(w_j^l)}{\sum_{j=1}^n \sum_{i=1}^m Attr_i(w_j^l)} \quad (18)$$

Let \mathcal{N} be the set of neurons classified as knowledge neurons based on their attribution scores exceeding a predetermined threshold τ , for a given input q . This can be formally defined as:

$$\mathcal{N} = \left\{ w_j^{(l)} \mid Attr(w_j^{(l)}) > \tau \right\} \quad (19)$$

where l encompassing all layers and j including all neurons within each layer.

A.5 Metrics for Knowledge Editing

In Table 2 and Table3, there are three indicators reliability, generalization, and locality, which represent the effect of knowledge modification. In fact, we are inspired by the field of knowledge editing [43], below we will give a complete introduction.

Model editing focuses on modifying the behavior of a base model f_θ (where θ represents the model parameters) given an edit descriptor (x_e, y_e) . The objective is to produce an edited model f_{θ_e} that incorporates the desired changes efficiently without affecting the model's performance on unrelated samples. The base model f_θ maps inputs to predictions:

$$f : \mathbb{X} \mapsto \mathbb{Y} \quad (20)$$

where x is the input and y is the corresponding prediction. The edit descriptor (x_e, y_e) specifies an input x_e and a desired output y_e . If the original model does not yield the expected output ($f_\theta(x_e) \neq y_e$), the post-edit model f_{θ_e} should return the correct prediction:

$$f_{\theta_e}(x_e) = y_e \quad (21)$$

The editing process generally affects predictions for a range of inputs closely related to the edit descriptor, termed the editing scope. A successful edit modifies predictions within this scope while leaving predictions outside it unchanged:

$$f_{\theta_e}(x) = \begin{cases} y_e & \text{if } x \in I(x_e, y_e) \\ f_\theta(x) & \text{if } x \in O(x_e, y_e) \end{cases} \quad (22)$$

where In-Scope ($I(x_e, y_e)$) comprises the edit input x_e and its equivalence neighborhood $N(x_e, y_e)$, which includes related input-output pairs. Out-of-Scope ($O(x_e, y_e)$) contains inputs unrelated to the edit descriptor. The edited model f_{θ_e} should satisfy three primary properties: reliability, generalization, and locality.

Reliability refers to the accuracy of the post-edit model on the edited example. Specifically, the post-edit model f_{θ_e} should reliably output the target answer for the edit descriptor (x_e, y_e) :

$$\mathbb{E}_{x'_e, y'_e \sim \{(x_e, y_e)\}} \mathbb{1} \{ \text{argmax}_y f_{\theta_e}(y \mid x'_e) = y'_e \} \quad (23)$$

Generalization measures how well the edited model adapts to equivalent neighbors within the in-scope neighborhood $N(x_e, y_e)$. The post-edit model should predict accurately on related examples:

$$\mathbb{E}_{x'_e, y'_e \sim N(x_e, y_e)} \mathbb{1} \{ \text{argmax}_y f_{\theta_e}(y \mid x'_e) = y'_e \} \quad (24)$$

Locality, also known as specificity, ensures that the edit remains local and does not affect the predictions for out-of-scope examples. Thus, the post-edit model should maintain consistency with the pre-edit model on unrelated examples:

$$\mathbb{E}_{x'_e, y'_e \sim O(x_e, y_e)} \mathbb{1} \{ f_{\theta_e}(y \mid x'_e) = f_\theta(y \mid x'_e) \} \quad (25)$$